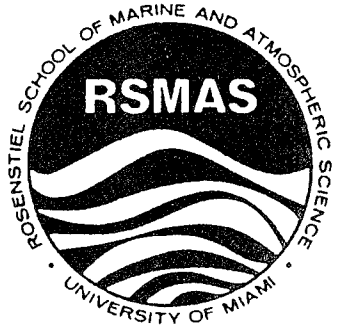

RSMAS 95-009

A LIGHTWEIGHT MULTI-SPAR BUOY
-- DESIGN AND SEA TRIALS --

by

Hans C. Graber[†], Eugene A. Terray[‡], Mark A. Donelan[§], John VanLeer[*] and William M. Drennan[§]

[†]Division of Applied Marine Physics
Rosenstiel School of Marine and Atmospheric Science
University of Miami
Miami, Florida 33149, USA

[‡]Department of Applied Ocean Physics and Engineering
Woods Hole Oceanographic Institution
Woods Hole, Massachusetts 02543, USA

[§]National Water Research Institute
Department of Environment
Canada Centre for Inland Waters
Burlington, Ontario L7R 4A6, Canada

*Division of Meteorology and Physical Oceanography
Rosenstiel School of Marine and Atmospheric Science
University of Miami
Miami, Florida 33149, USA

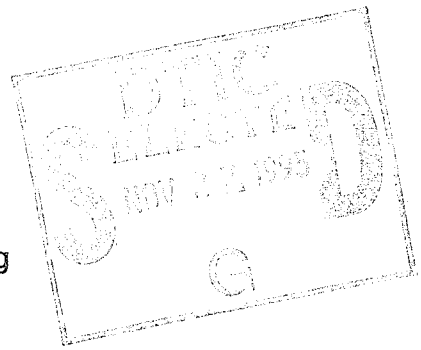

October 1995

Technical Report

Approved For Public Release; Distribution Is Unlimited.

Prepared for OFFICE OF NAVAL RESEARCH
Under ONR contract N00014-91-J-4142

DISCLAIMER NOTICE

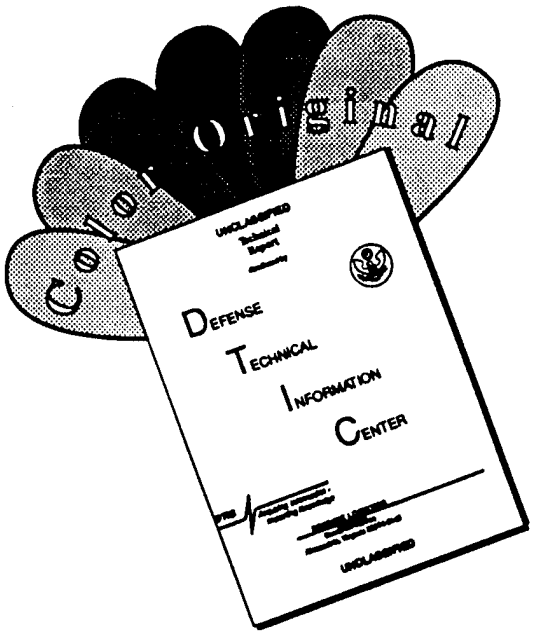

THIS DOCUMENT IS BEST QUALITY AVAILABLE. THE COPY FURNISHED TO DTIC CONTAINED A SIGNIFICANT NUMBER OF COLOR PAGES WHICH DO NOT REPRODUCE LEGIBLY ON BLACK AND WHITE MICROFICHE.

RSMAS 95-009

A LIGHTWEIGHT MULTI-SPAR BUOY
-- DESIGN AND SEA TRIALS --

by

Hans C. Graber[†], Eugene A. Terray[‡], Mark A. Donelan[§], John VanLeer[*] and William M. Drennan[§]

[†]Division of Applied Marine Physics
Rosenstiel School of Marine and Atmospheric Science
University of Miami
Miami, Florida 33149, USA

[‡]Department of Applied Ocean Physics and Engineering
Woods Hole Oceanographic Institution
Woods Hole, Massachusetts 02543, USA

[§]National Water Research Institute
Department of Environment
Canada Centre for Inland Waters
Burlington, Ontario L7R 4A6, Canada

[*]Division of Meteorology and Physical Oceanography
Rosenstiel School of Marine and Atmospheric Science
University of Miami
Miami, Florida 33149, USA

October 1995

Technical Report

Approved For Public Release; Distribution Is Unlimited.

Prepared for OFFICE OF NAVAL RESEARCH
Under ONR contract N00014-91-J-4142

Table of Contents

List of Tables

List of Figures

Preface

The authors gratefully acknowledge funding support by the Remote Sensing Program (Code 1121RS) and the Office of Naval Technology at the Office of Naval Research (ONR) under Grant No. N00014-90-J-1464.

The authors extend special thanks to Melbourne G. Briscoe (formerly at ONR), NOAA, who saw the need of such a measuring system for acoustic surface reverberations and Marshall Orr (formerly at ONR), Naval Research Laboratory, who supported the initial developing of this concept under the Acoustic Surface Reverberations Program. Steve Ramberg and Frank Herr (ONR) saw the potential of this innovative buoy concept and provided the support to start the development and fabrication of the MultiSpar buoy and Dennis Trizna maintained a continuous interest throughout the development stages.

The authors thank the following personnel for the long hours and hard in work preparing for and successfully completing these sea trials: Mike Rebozo, Louis Chemi, John Hargrove and Ram Vakkayil (RSMAS), Ken Prada, Neil McPhee, Don Peters and Mark Grosenbaugh (WHOI), Manuel Pedroza and Joe Gabriele (CCIW), the personnel of the Mechanical Shop at WHOI and the crew of the *M/V Seaward Explorer*.

1 INTRODUCTION

There is a growing need for high resolution wave directional measurements at sea, arising in diverse fields such as wave dynamics, microwave and acoustic remote sensing, air-sea coupling and gas transfer. In most research investigations in these areas it is desirable (and often critical) to make measurements of relevant quantities (*i.e.* of environmental parameters) at the air-sea interface coincident in time and space with the particular process under study. Examples are wave directional and probability structure with acoustic or radar signatures of breaking; wave steepness, breaking and bubble distribution with gas transfer; wave growth with momentum transfer from the surface wind stress.

The availability of a ***general purpose lightweight spar*** with wave and flux measurement capability would significantly enhance experimental research of air-sea interaction, wave dynamics, acoustic and microwave remote sensing and gas transfer. The flexible design concept of this spar buoy is amenable to measurements in the open ocean, in boundary currents, on the continental shelf and in coastal waters.

The spar buoy is designed to function in two deployment modes. When deployed as a drifting instrument, this buoy would monitor wave properties, the dissipation and mixing rates and marine surface fluxes, *inter alia*, at the air-sea interface as a function of position and time. Within current systems such as the Gulf Stream we could obtain valuable new information on wave-current interaction and the modified properties of the wave field and overlying marine boundary layer characteristics. In its moored configuration, this buoy would yield measurements over extended periods. For example, high resolution wave directional measurements are required for making further advances in microwave remote sensing, gas transfer and acoustic studies. Wavestaff spacings of a centimeter or less are possible using thin wires under high tension. More sophisticated and durable methods (for example, using low-powered lasers) will be evaluated and, as the technology develops, will replace the thin wires. Principal research interests in these short gravity waves are found in the fields of acoustic and remote sensing because they are responsible for Bragg scattering of acoustic and microwave radiation.

Sufficiently long waves propagating over variable bottom topography are altered in height, period and direction due to interactions with the ocean bottom (*e.g.*, Graber *et al.* 1990; Graber *et al.* 1991). At present we lack complete understanding of the impact of depth refraction on wave spectral evolution and which spatial scales of the bottom variability are important. In contrast, shear and vorticity in the horizontal surface currents as found in Gulf Stream fronts, filaments, eddies and rings can modify the wave characteristics over a wide range of frequencies. Especially focusing of rays can lead to caustics which promote breaking (*e.g.*, Shay *et al.* 1995; Walsh *et al.* 1995). For either situation, an array of these spar buoys would provide high-resolution and accurate directional wave characteristics and the spatial gradients to determine the rates of change in wave properties due to wave-bottom and/or wave-current interactions. Therefore, the focus for the design of an appropriate buoy system was the measurement of wave

directional spectra at high resolution. This may be done in principle with a wide range of possible sensor technologies including wave staffs, pressure transducers, current meters, slope following devices, laser elevation or slope gauges, acoustic or electromagnetic ranging devices etc.

The initial motivation for the development of the MultiSpar buoy was the measurement of direction for waves with frequencies about 2 Hz and below. This portion of the spectrum was identified by the *Acoustic Reverberations Special Research Program* as possibly an important mechanism for the Bragg-scattering of sound with frequencies below approximately 500 Hz. Subsequently, one of the scientific goals of the *Surface Wave Dynamics Experiment* (SWADE) was on the effect of waves on the air-sea transfers of momentum, heat and mass and the stability effects on the flux-profile relations (Weller *et al.* 1991). To achieve this goal further advancement in the analysis and interpretation of the directional wave spectrum, specifically its evolution, relaxation to equilibrium and response to wind changes and current shears, are necessary. For example, more accurate and denser measurements are crucial to improving model physics and methodologies in numerical modelling (Cardone *et al.* 1995). SWADE was followed by the *High Resolution Remote Sensing Program* (HIRES) which specified that better knowledge of the modulation of wave frequencies in the range of 2-5 Hz in the presence of mesoscale features is essential in understanding the modulation of the Bragg-scattering waves and hence the radar backscatter (Herr *et al.* 1991). Precise interpretation of radar and acoustic backscatter in the context of improved understanding of the Bragg-wave modulation is a critical step in the evaluation of radar images and acoustic signatures of mesoscale ocean features.

2 BUOY SYSTEM DESIGN

2.1 The MultiSpar Buoy

The criteria we used to develop this buoy system are the following:

(a) *High resolution directional wave spectra.*

(b) *Ease of adjustment of Nyquist wavelength - i.e. array dimensions can be changed readily, and more complicated arrays should be possible without major modification to the buoy design.*

(c) *Surface-following for long waves - this is particularly important when measuring wind-wave spectra because of the typically large range of amplitudes present in the wave field.*

(d) *High accuracy air-sea mean and flux measurements - requiring low flow disturbance.*

(e) *Suitable platform for a wide range of (passive) measurements within 1 meter of the interface.*

(f) *Sufficient vertical stability to facilitate active acoustic and microwave remote sensing measurements.*

(g) *Adaptability to both deep and shallow (< 20 m) water depths and to mooring and drifting configurations.*

(h) *Ease of deployment, retrieval, maintenance and long term durability in harsh environments.*

(i) *Reasonable cost (comparable to off-the-shelf pitch-roll or waverider buoys).*

To meet these objectives outlined above, we have chosen to design the buoy as a short spar. However, instead of intersecting the surface as a single column, we use a pentagonal cage of slender cylinders separated by several meters. This design concept distributes the buoyancy of the members around the perimeter rather than in a single pole. While long single spars (*e.g.*, FLIP) are very stable platforms well below their resonance period, they may be excited in pitch and roll near resonance (Berteaux and Walden 1978). In contrast, the multi member spar design is an overdamped system with increased stability to pitch and roll. In addition, the smaller cylinder dimensions serve to reduce flow distortion in the vicinity of the buoy (Zdravkovich 1981). The prototype buoy uses a compact array of capacitance wave staffs located inside and along the perimeter of the cage to measure wave elevation. The motion of the buoy is sensed by a motion-package consisting of orthogonal triplets of both linear accelerometers and rate gyros, together with a 3-axis magnetometer. All of these sensors are "strapped-down", avoiding additional dynamical uncertainties inherent in gimbaled designs. By measuring both the buoy motion and the position of the surface relative to the buoy, we eliminate the need to control or

have *a priori* knowledge of the response function of the platform for data analysis. The spar, which we have named a **MultiSpar buoy**, can be freely drifting or laterally tethered to a surface mooring (the **tether buoy**), which itself can carry both air- and water-side sensors and telemetry. Figures 1 and 2 show the prototype MultiSpar buoy.

To guide the longterm design and refinement of the MultiSpar we have developed numerical models for the hydrodynamics. These models will be refined by assimilating the field measurements of the response of the spar to wave forcing. During the field performance tests, detailed measurements of the motion of the spar and the waves were made to evaluate the buoy's response in heave, pitch, roll, sway, surge and yaw and to correct the relative-to-buoy environmental measurements of acceleration, velocity and displacement.

Criteria (a) to (c) led to a short multi-spar with good vertical stability. The choice of surface intersecting wave staffs within a protective cage permits very flexible choices of Nyquist wavelength, which determines the size of the inscribed centered pentagon of staffs, while the largest observable wave length is determined by the slope quantization level. The principal disadvantage of wave staffs is that they will need periodic cleaning, but the size of buoy allows reasonably easy crane pick up and retrieval to ship-deck. The buoy is designed so that additional buoyancy sections and ballast may be added to tune its surface following characteristics.

A number of sea trials have been conducted in the North Sea with a buoy similar in concept to the MultiSpar, but tethered to a ship (Crowther and Perry 1970). Although the duration of making useful measurements in such a configuration is limited, the directional wave measurements were far superior to those from a conventional pitch/roll buoy (Figure 3).

In addition, design considerations are given to mount a microwave radar on the mast for in-situ measurements of backscatter. For such observations, a second centered pentagon of wave staffs could be added to measure the directional wave field and its slopes at two different spatial resolutions (Figure 4). In particular, the second wave staff array could be tuned to the Bragg resonant wave lengths of the radar. For these relatively high frequency waves, the buoy response will be small and measurements of wave height are essentially equivalent to those in a fixed reference frame. This is illustrated in Figure 3 which shows wave height and first-difference spectra measured by a 3-element wavestaff array mounted on a short spar of the general type under discussion here (the natural period of this particular buoy was about 15 seconds). The height spectrum exhibits a relatively well-developed "equilibrium range" (the slight aliasing at high frequencies is a consequence of the 10 Hz sampling rate), while the first-difference spectrum has the expected slope of -1/2 (for wavenumbers below the spatial cutoff of the array) - both of these features are in agreement with fixed array observations.

In contrast, estimating the direction of low-frequency waves is complicated both by the fact that their slopes are smaller, and by the response of the spar at low frequencies - which will be designed to approximately follow the long waves. The quantization error over a 2

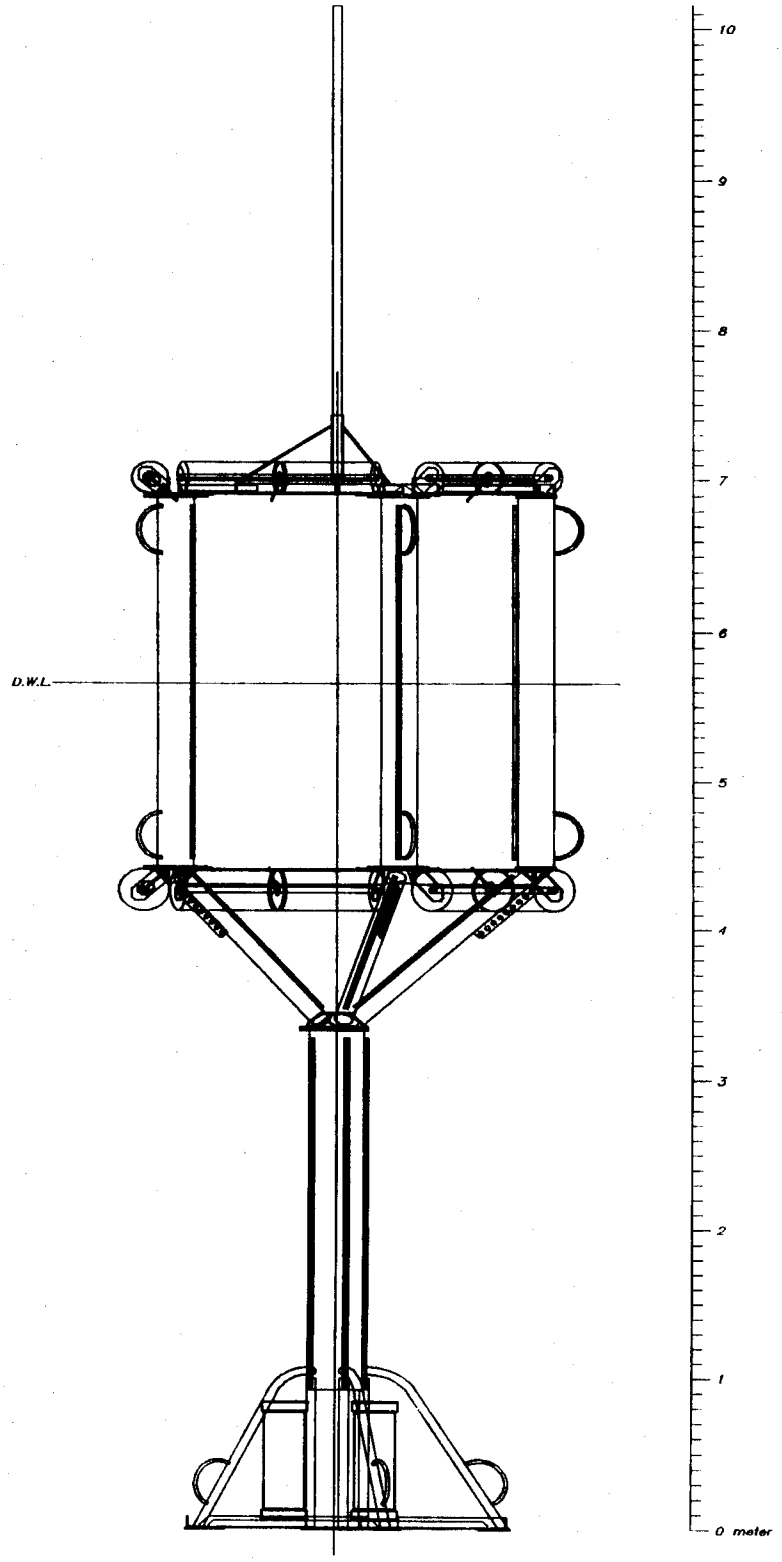

Figure 1: Engineering drawing of prototype MultiSpar buoy.

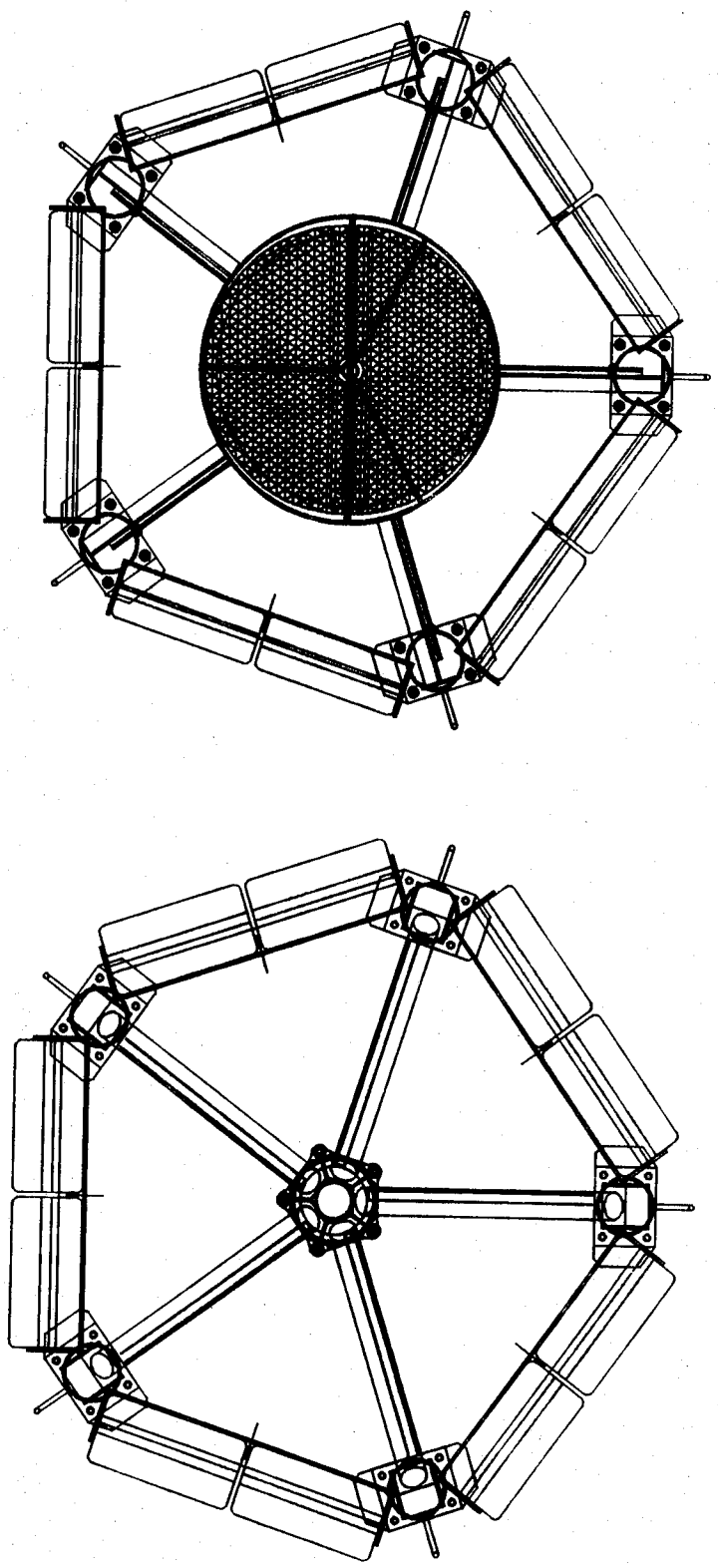

Figure 2: Plan view of prototype MultiSpar buoy.

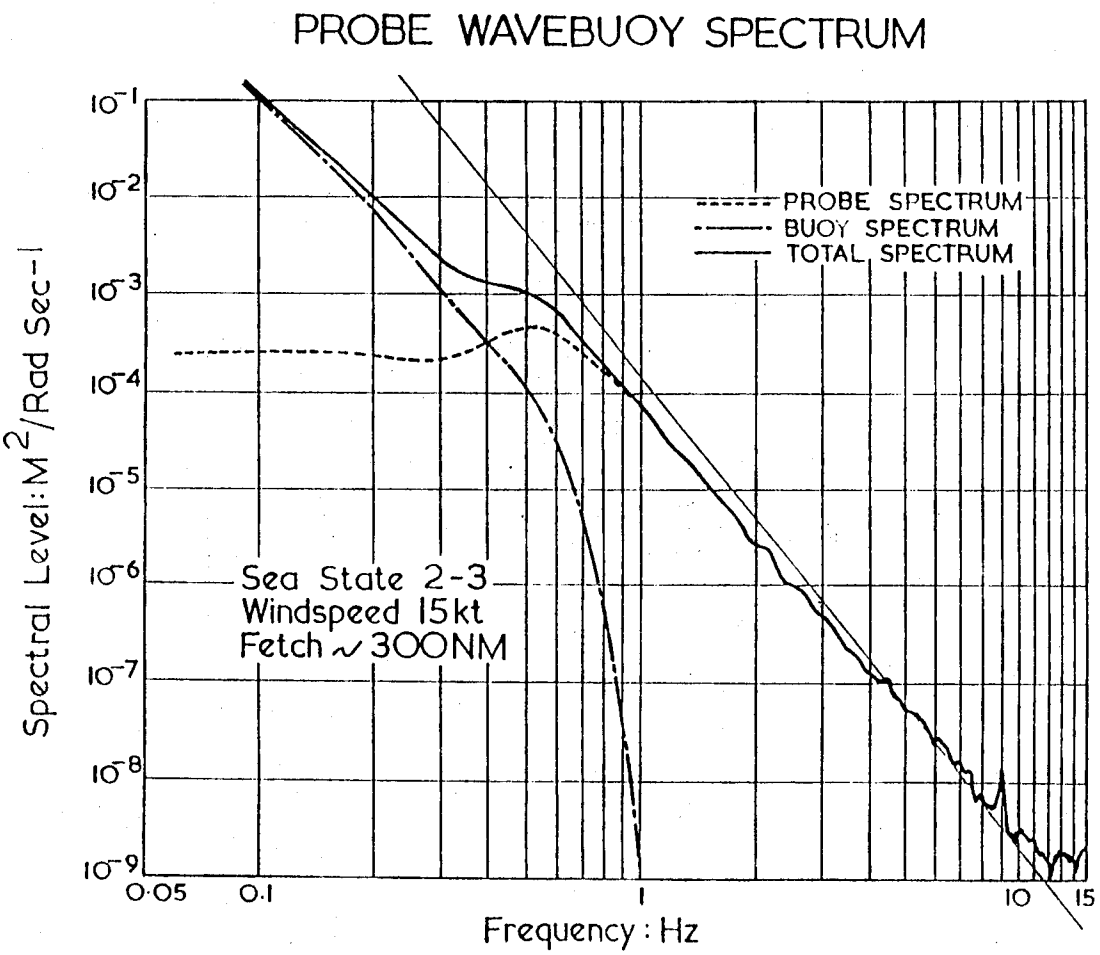

Figure 3: Comparison of wave spectra as measured by pitch/roll and probe buoys (Crowther and Perry, 1970).

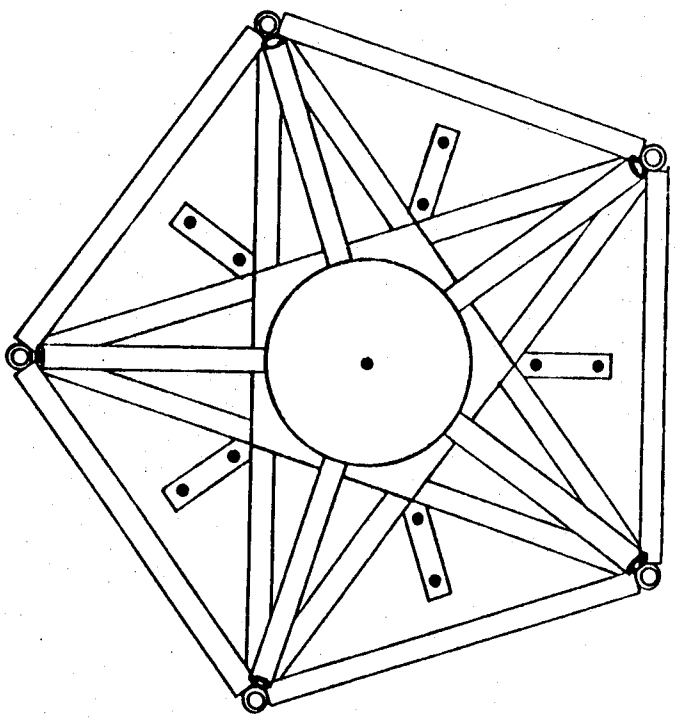

Figure 4: Geometric configuration of two centered pentagon wave staff arrays with different spatial resolution.

m wavestaff (assuming 12-bit resolution) permits slope measurements to approximately 10^{-3} for an array with a maximum spacing of 1 m. For a 20 s, deep-water wave, this translates into a minimum resolvable amplitude of 5 cm. Waves with such small slopes are unlikely to be dynamically important either as a direct acoustic scattering mechanism or in modifying the properties of shorter waves. However, if necessary, smaller slopes can be resolved using a larger array spacing. A more serious consideration is the precision to which the buoy motion is known. Although a variety of approaches to this problem can be taken, for the spar a combination of 3 linear plus 2 rotational accelerometers is prefered since: (1) they have low power consumption, and (2) will permit a relatively compact motion-sensing package. Rotational accelerometers are presently available that are extremely insensitive to linear accelerations (< 5 mrad s^{-2} g^{-1}), yet have sufficient dynamic range and sensitivity to measure the expected pitch and roll motions of the spar. For very long periods (> 15 s) the buoy may be treated as a floating particle and the directional properties of these waves measured from the three components of linear acceleration (or velocity, or displacement).

Figure 5 shows the prototype MultiSpar buoy in its configuration for the sea trials, in which it was equipped to measure the momentum flux using a sonic anemometer and a nested wave staff array. The technology for such measurements of fluxes and wave properties from moving platforms was developed for the ONR programs SWADE (*Surface Wave Dynamics Experiment*) and HIRES (*High Resolution Remote Sensing Experiment*) (*e.g.*, Katsaros *et al.* 1993, Anctil *et al.* 1994 and Drennan *et al.* 1994).

2.2 The "Tether" Buoy

Although the spar by itself would provide an almost ideal surface platform when freely drifting, it is important in many applications that long time series be obtained from a single location. For this reason, the issue of the spar mooring is fundamental to this project. The small waterplane area of the spar implies a relatively small reserve buoyancy, and consequently it is important to avoid the additional downward forces generated by a subsurface anchor - which can vary widely depending on the current environment. - and to attach the spar to a surface mooring by means of a buoyant tether. The tether was constructed of closed cell Surlyn Ionomer foam, and designed insofar as possible to operate in a region of approximately linear response (the latter will simplify the transfer function of the combined spar/tether system). The foam construction yields also a self fendering type of buoy which can minimize the impact of a collision. Pigment, anti-oxidant, anti-UV and anti-fouling compounds were added to the finished buoy. The use of a surface mooring has other advantages in that it can carry additional surface and subsurface instrumentation, such as solar panels and thermistor strings, and can be used (in conjunction with an umbilical cord or an RF link to the spar) for tasks requiring high power or recharging capabilities, such as data storage and long-range telemetry.

Various options for the tether buoy were explored. In particular, most traditional buoys have been built with exoskeletons such as hard exterior steel or fiberglass shells which give the buoy its form and strength as well as resistance to damage. These buoys are built

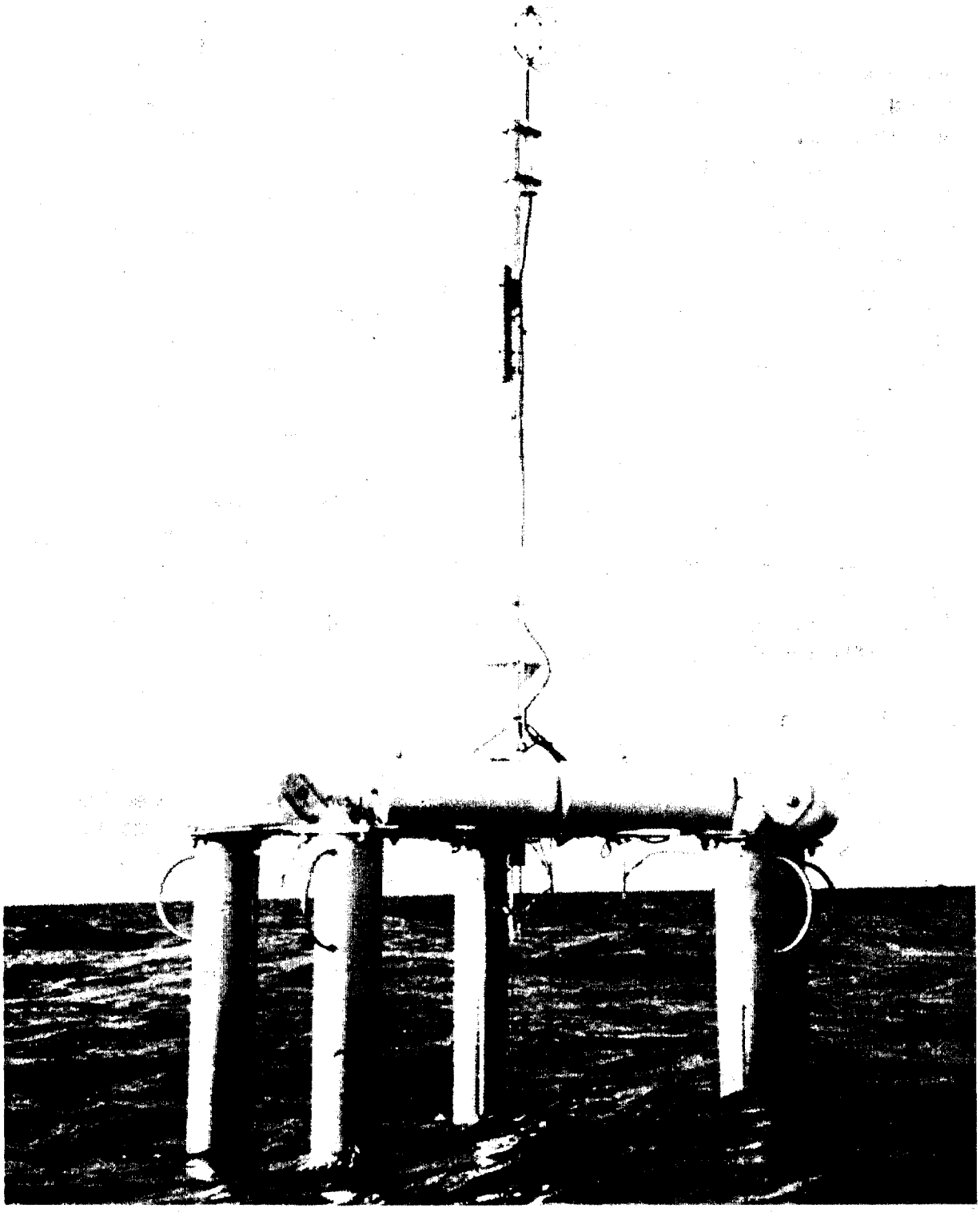

Figure 5: Prototype MultiSpar buoy deployed at sea.

with readily available ship building techniques and are typically heavier and less expensive to construct (Steele *et al.* 1992).

However, with todays rugged ionomer foam floatation, an aluminum endoskeleton can be built which handles all structural functions and can be surrounded by a collar of foam serving as both floatation and fender. This technique yields a lighter weight but more expensive buoy with lower maintenance costs since the surface skin is formed out of foam and does not require repainting. However, the most important aspect of the foam buoy designed by RSMAS was the availability of over 11,000 pounds of buoyancy!

Additional concerns arose due to the possibility of entanglement of the buoy and its tether. To avoid entanglement, the tethered MultiSpar buoy must be free to move in any direction without wrapping the tether around the Tether buoy. The tether must be decoupled in rotation from the tether buoy by means of a low friction swivel located below any instrumentation on the tether buoy. A "tether lever" extending beyond the main body of the tether buoy has been used successfully at RSMAS to provide enough excess torque to guarantee revolution of a rotationally symmetric Tether buoy without wrapping up the tether even in weak currents. Table 1 shows design and functional attributes of two contrasting Tether buoy shapes.

Table 1
Attributes of Tether Buoy Shapes

Attribute	Cylindrical	Spherical
Displacement	8.5 m^3	8.5 m^3
Tether Lever	Fixed to top plate	Fixed to mid plate
Entanglement potential of tether	Unlikely with floating at mid hull with constant radius	More likely if tether wraps below equator on narrowing radius
Buoy Motion	Hull shape generates restoring force with pitch and roll motions	Hull shape generates no restoring force with pitch and roll motions
Ballast Requirements	Requires less ballast due to hull stability	Requires more ballast to make up for lack of hull stability
Cost of Construction	Cylinder is cheaper to form in metal or foam	Sphere is more expensive to form in metal or foam
Solar Panel Placement	Solar panel may be placed on flat deck	No natural flat upward surface except mast top

Since the MultiSpar buoy will have limited reserve buoyancy, a buoyant tether was chosen to avoid significant downward forces on it. Furthermore, to minimize any additional downward pull on the MultiSpar, we attached the surface tether to a lever extending from the Tether buoy above the waterline. This arrangement served a second purpose,

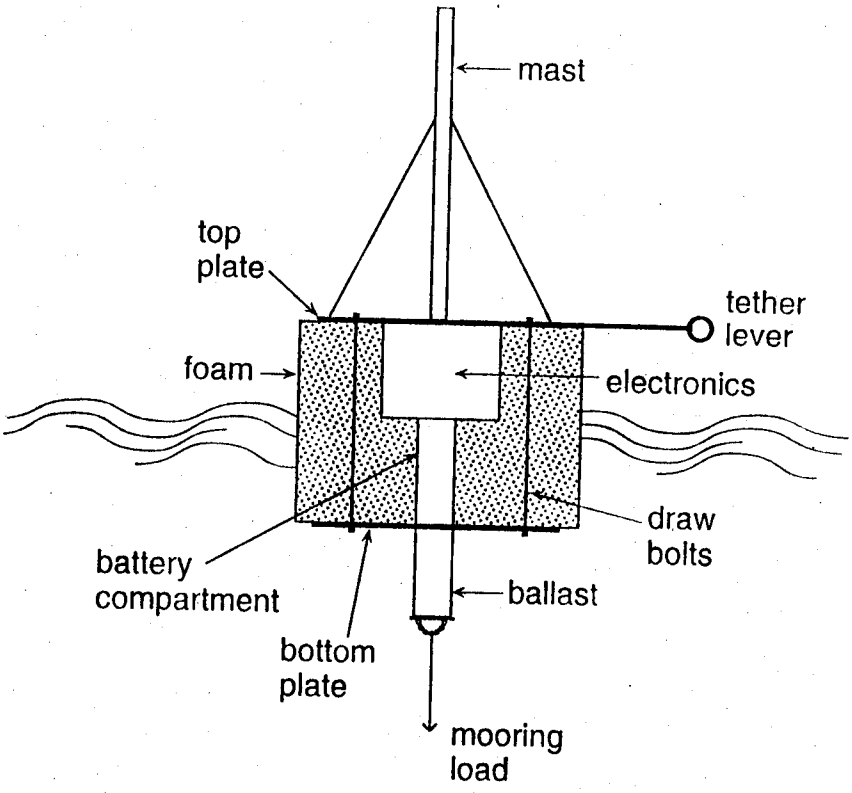

Figure 6: Schematic design of Tether buoy.

especially during launching and retrieval operations. In this way the Tether buoy could be launched and anchored first, and then the MultiSpar buoy could be towed by the surface tether with a small boat, the tether is then connected to the lever. Figure 6 illustrates the schematic design of the Tether buoy used for the MultiSpar-Tether buoy system.

3 PERFORMANCE AT SEA

To test the behavior and performance of the spar/tether buoy system in typical oceanic and atmospheric conditions, a four day engineering and sea trial test was conducted at a site in about 50 m water near the US Coast Guard Lighthouse *Fowey Rocks* which also serves as a station in NOAA's Coastal Marine Automated Network (C-MAN). This site was selected for several reasons: (1) it is exposed to the open ocean, where wind waves along fetches from north to south approach the coastline and (2) it is shoreward of the Florida Current, which frequently sheds spin-off eddies that propagate along and onto the shelf (Lee *et al.* 1975) and induce moderately strong current flows which are tidally modulated.

The sea trials were conducted from 4 - 7 May, 1994. First the Tether buoy without the surface tether was deployed. The anchor of the tether buoy, a cluster of five railroad wheels, was dropped at 25° 35' 33" N, 80° 05' 28" W, about 1 km east-northeast of *Fowey Rocks*. Next we deployed the multi-spar without instrumentation to test (1) its sea worthiness, (2) response to pitch and roll, and (3) the ease of launching and retrieving the buoy. Simple rocking tests were performed to observe the buoy's motion response at sea and its capability to restore and align itself vertically. Figure 7 depicts the the MultiSpar buoy on deck of the *M/V Seaward Explorer*.

The MultiSpar was fully deployed on 6 May with the following instrumentation configuration: a nested wire wave gauge array, a sonic anemometer and a motion sensing package. With an inflatable zodiac the MultiSpar was towed on its surface tether to the Tether buoy and fastened to the tether lever.

Data collection continued for about 18 hours until the buoy system was recovered on 7 May. The ship's anemometer indicated winds from the east at around 11 to 15 knots. Seas of about 60 to 100 cm were estimated at this time by visual observations. The launch and retrieval of the MultiSpar system was found to be relatively easy. Figure 8 shows the full MultiSpar-Tether buoy system deployed at sea.

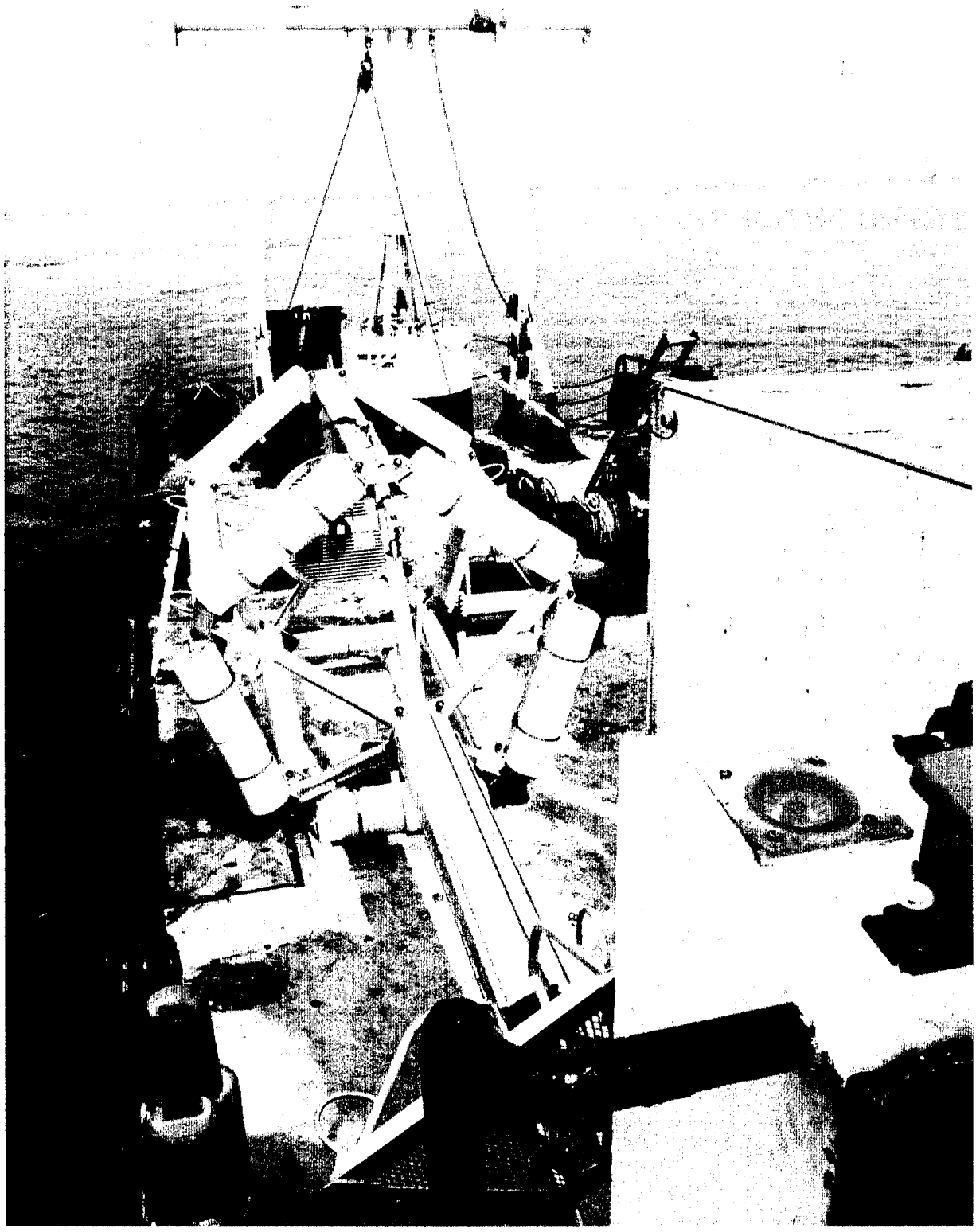

Figure 7: MultiSpar buoy on deck of the *M/V Seaward Explorer.*

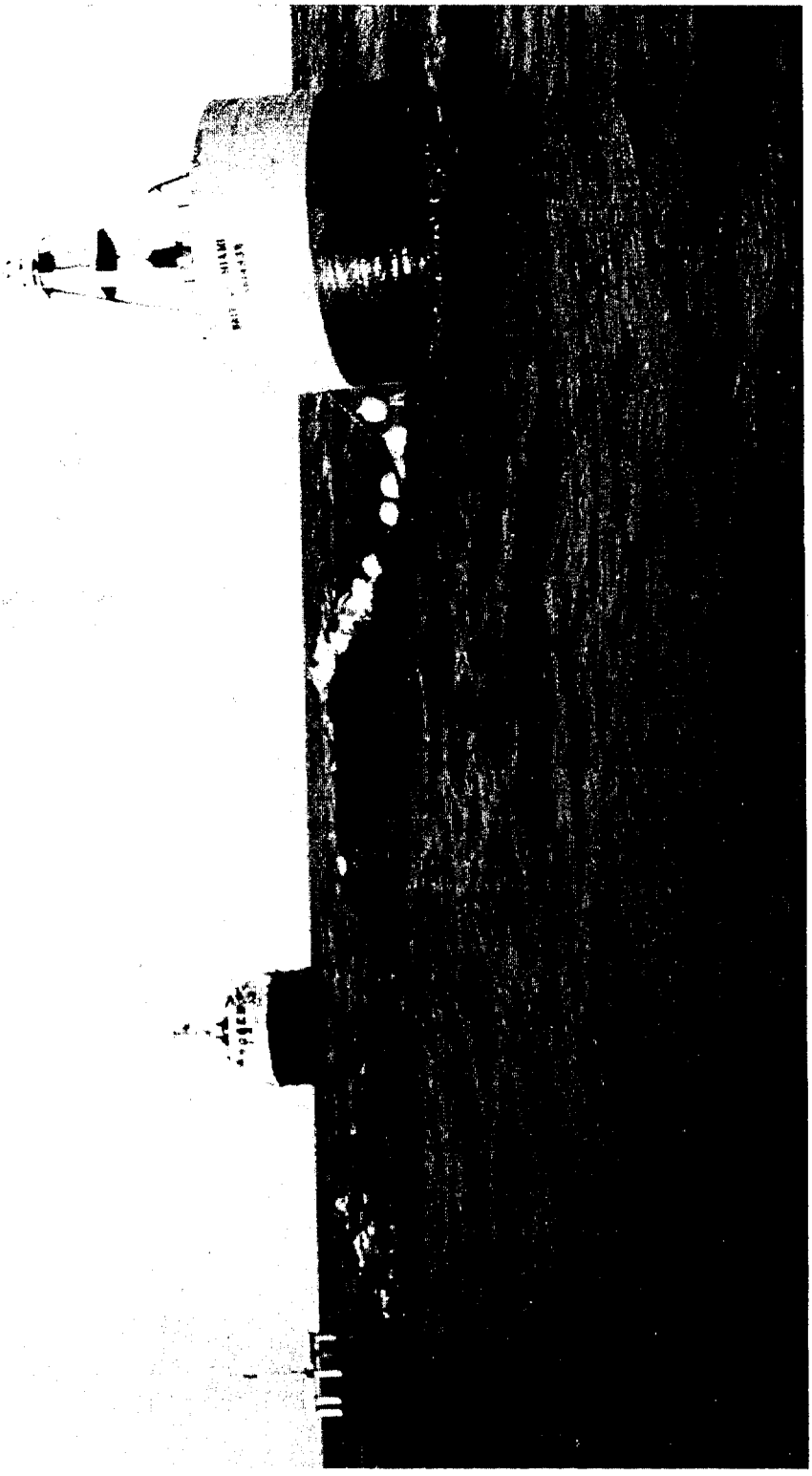

Figure 8: MultiSpar-Tether buoy system deployed at sea of *Fowey Rocks* Lighthouse.

4 INSTRUMENTATION

4.1 Motion Sensors

Table 2 presents a summary of the sensors deployed on the MultiSpar during the sea trials. The translational and rotational motion of the buoy is measured in all six degrees of freedom. Linear accelerations are sensed by tri-axial force balance accelerometers. These are three independent orthogonal acceleration sensors in a single package. The unit used is model number SA-307HPTX, manufactured by Columbia Research Labs Inc. The vertical component is "g-biased", *i.e.* reads zero when at rest in a gravitational field g = (0, 0, -9.806 m s^{-1}). The three axes have a nominal range of $\pm\frac{1}{2}$g corresponding to $\pm$5 volts.

Rotational motion is sensed by three solid state angular rate sensors. These "Gyrochips" use a quartz crystal oscillator whose frequency is proportional to angular velocity about an axis. These are mounted along the three orthogonal axes of the linear accelerometers and have a nominal range of $\pm 20°s^{-1}$ corresponding to $\pm$2.5 volts. Pitch and roll angles are obtained by integrating the appropriate pitch and roll rates once with a low frequency cut-off of 0.025 Hz, *i.e.* motions with periods greater than 40 seconds are assumed negligible. The integration of yaw rate provides yaw angle fluctuations at frequencies greater than 0.025 Hz. Lower frequency fluctuations are provided by a Develco flux-gate magnetometer.

These seven sensors together yield all the required information on the motion of the buoy. This is a "strapped down" system, which is to say that the variables are measured with respect to a coordinate system fixed in the buoy. In order to obtain the "earth referenced" motion of the buoy, various coordinate transforms (Anctil *et al.* 1994 and Katsaros *et al.* 1993) need to be applied. The approximation used, *i.e.* that the measured angles may be taken as Euler angles, is accurate for small angle fluctuations such as those experienced by the MultiSpar (see below).

Table 2
Equipment Deployed during Sea Trials

Sensor	Manufacturer	Units
Linear accelerometer	Columbia Research Lab. SA-307HPTX	3
Gyrochips	Systron-Donner	3
Magnetometer	Develco Fluxgate	1
Wave staffs	NWRI	8
Sonic anemometer	Gill Solent	1

4.2 Wind and Wave Sensors

The wind sensor selected is a state-of-the-art acoustic velocity component anemometer-thermometer. Acoustic anemometry has been used for meteorological research for about thirty years. It is the method of choice for both mean and fluctuating values. Its calibration is established by its geometry and the speed of sound in air, itself a weak function of temperature in the normal run of temperature fluctuations in air. The development of the Solent Anemometer has dramatically widened the use of these devices for autonomous long term recording in hostile environments. The Solent 3-axis anemometer-thermometer weighs 1 kg, consumes 1 watt of power and works reliably for long periods. The sample rate for all paths is 168 Hz and we record the filtered analog output at 20 Hz. The act of applying power to the instrument initiates a short calibration sequence of the DTOA converters on all four channels.

These anemometers are made in two configurations: (i) the *symmetrical design*, in which the passage of air through the sensed volume is interrupted by three slender vertical rods symmetrically placed around the perimeter; *i.e.*, at spacings of 120°; (ii) the *asymmetrical design*, in which the three slender rods are only 60° apart so that the "throat" is 240° wide. In both cases the instruments are individually calibrated in a wind tunnel and delivered with an azimuth dependent calibration table that corrects for wake effects from the support rods and transducers for steady flow. These corrections are very small for wind directions within $\pm 100°$ of the centre of the throat for the asymmetrical design. In our application the buoy is tethered and points into the resultant of wind and current forces, so that our choice of the asymmetrical head increases the likelihood of unimpeded flow through the sensor.

The wave sensors are capacitance wires of a design developed at the National Water Research Institute. In the initial tests of the spar buoy eight wires were installed with six in a centered pentagon configuration with a radius of 92.7 cm. The two additional wires were placed 2.86 cm from the centre wire to form a right isosceles triangle. The centered pentagon provides uniform directional sensitivity for the waves of length 185 cm and more. The isosceles triangle gives the directional properties of shorter waves in the range of wavelengths of 5.7 cm to 185 cm. In addition, the linear triangle can be used to measure two orthogonal components of the slope for all but the shortest waves.

5 RESULTS

5.1 Performance characteristics

The six degrees of freedom of the buoy's motion are continuously monitored and recorded at 20 Hz. The surface displacement (at 8 points) and the three components of wind velocity, relative to the buoy's position and velocity, are continuously recorded at 20 Hz also. Consequently, we can recover both the buoy's response and the principal forcing variables, i.e. waves and wind. In this section, we examine the transfer function that relates the response to the forcing.

Figure 9 shows an example of the surface displacement spectrum. The buoy's vertical displacement has been added to the relative displacements observed by the central wave staff to yield true surface elevation in the pass-band of 0.025 Hz to 10 Hz. The spectra are plotted on linear axes in the top panel of Figure 9 and on logarithmic axes in the bottom panel. The response closely follows the forcing between 0.1 and 0.17 Hz (10 to 6 second period), after which the response quickly drops off. This is more clearly seen in the top panel of Figure 10 in which is plotted the coherence and phase angle between the waves (forcing) and heave displacement (response). The coherence is high between 0.1 Hz and 0.6 Hz. In this region the phase rises to almost 60° at 0.2 Hz and drops off to near zero at higher frequencies. The corresponding amplitude transfer function is shown in the bottom panel (Figure 10). Only in the region of high coherence is this function meaningful. The response overshoots at 0.105 Hz and then quickly drops off at lower and higher frequencies. At 0.25 Hz and above the response is below 20%. Thus the buoy follows the longer waves and damps out the forcing for shorter waves, those with a wavelength less than 25 m.

The time series of the three linear accelerations (heave, surge and sway) are displayed in Figure 11. All three components have the same character and magnitude. Surge is in the direction of the tether or at about 45° to the wind direction. Consequently equal response in surge and sway is to be expected. It would seem that in these longer waves the buoy is moved around with the orbital velocities. It is particularly interesting that there is no evidence of jerking from the tether on the surge record.

We turn now to the angular motion of the buoy. Pitch, roll and yaw are displayed in Figure 12. The standard deviations of these are respectively 0.72, 0.67, 1.36 degrees. By comparison, a NDBC 3-m Discus buoy moored in somewhat calmer conditions (H_s = 62 cm, U = 5 m s^{-1}) during HIRES-2 experienced rms motions of 1.76, 2.01 and 5.50 degrees in pitch, roll and yaw, respectively. This represents an improvement in vertical stability of about a factor of three. These angles attest to the success of the MultiSpar in maintaining vertical stability. However, in order to see how well the buoy performs we need to compare the observed pitch and roll with the slope of the water surface in those directions (i.e. the forcing). We have estimated the surface slope across the buoy using the five wave staffs on the perimeter. The components of slope in the pitch (tether direction) and roll directions are shown in Figure 13. The corresponding coherences and

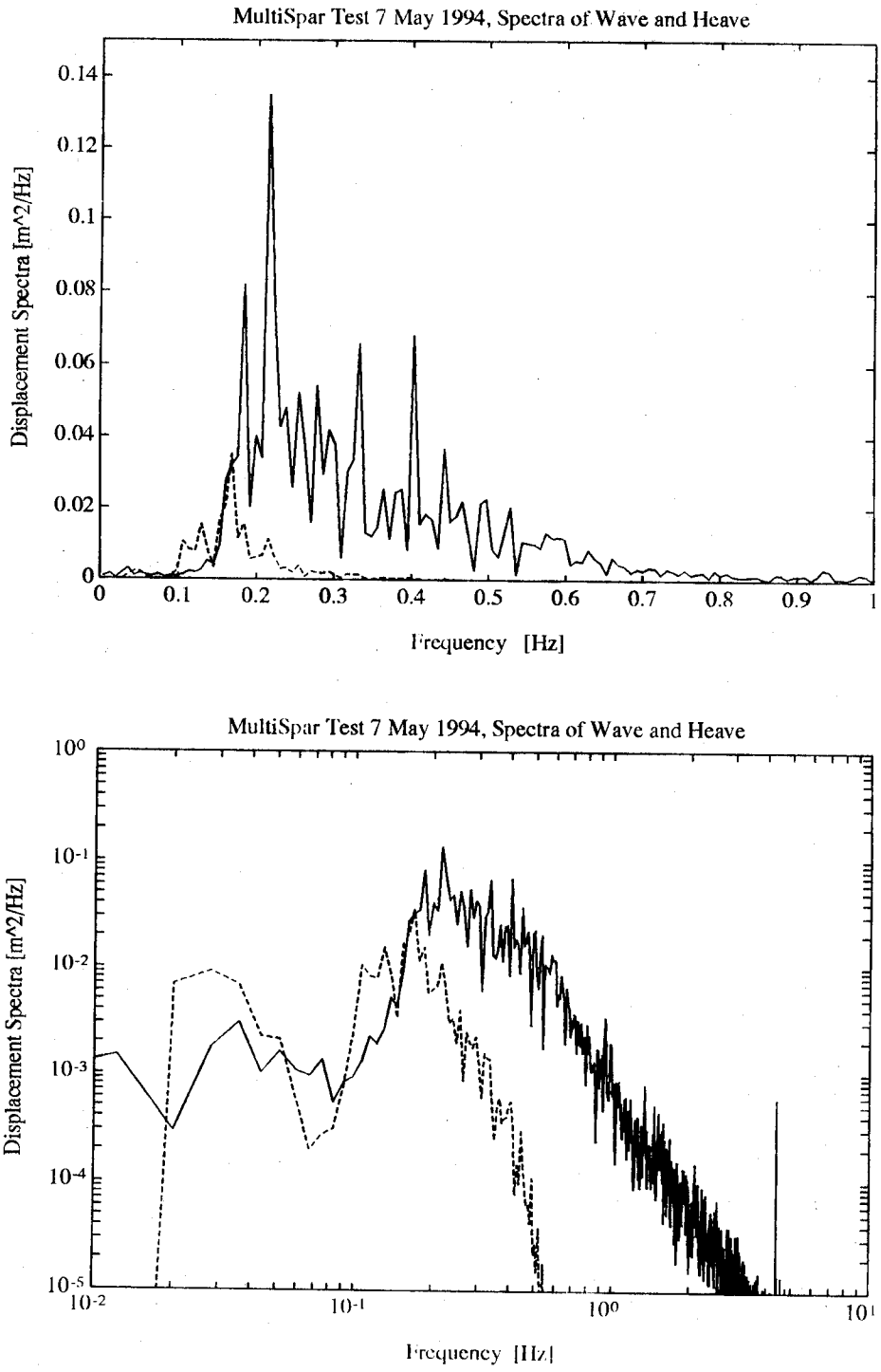

Figure 9: Surface displacement spectrum measured with MultiSpar buoy. The solid line is the wave energy spectrum and dashed line is the heave spectrum of the buoy.

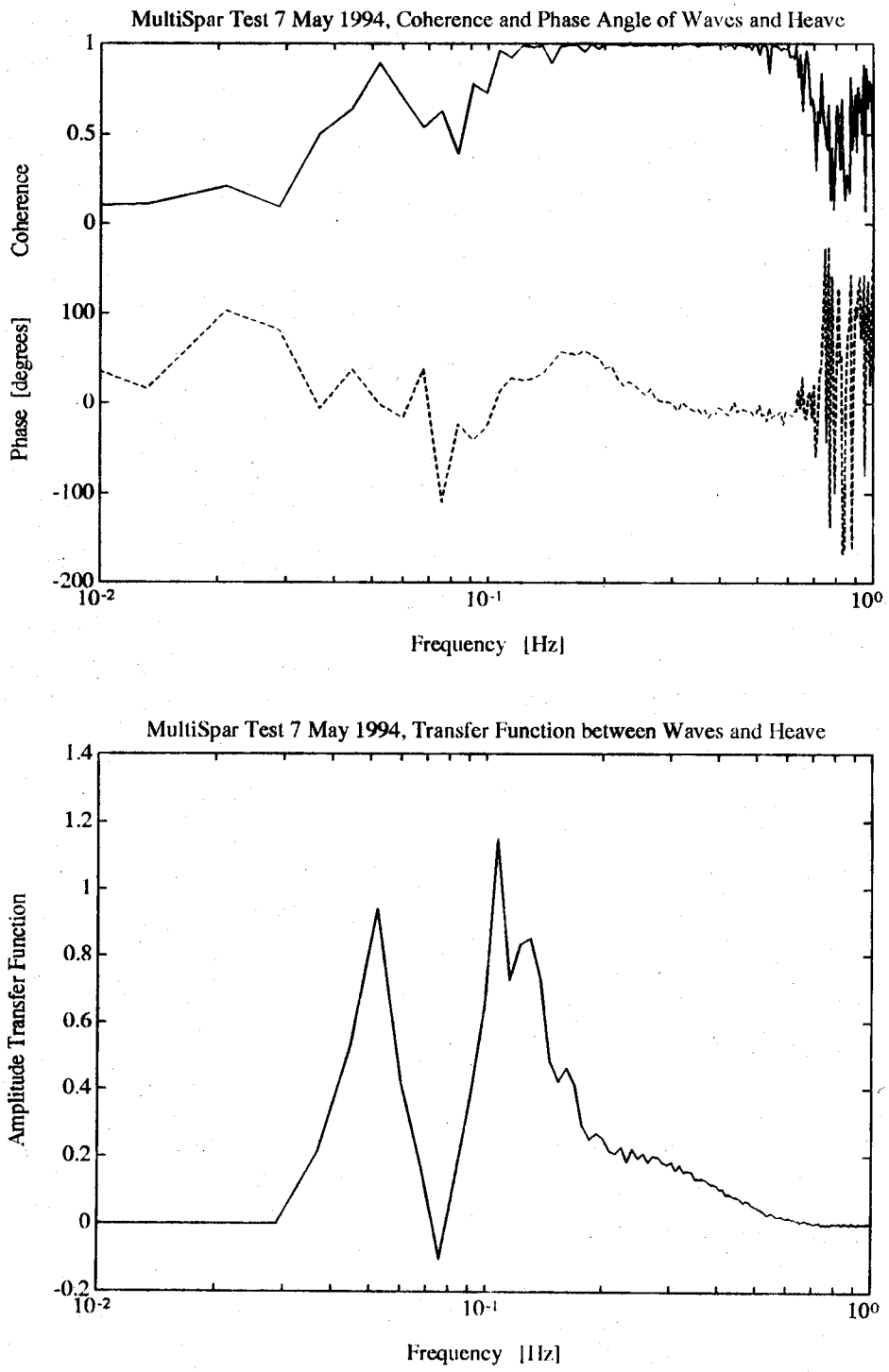

Figure 10: Coherence and phase angle between wave forcing and heave response (top panel) and the amplitude transfer function (bottom panel).

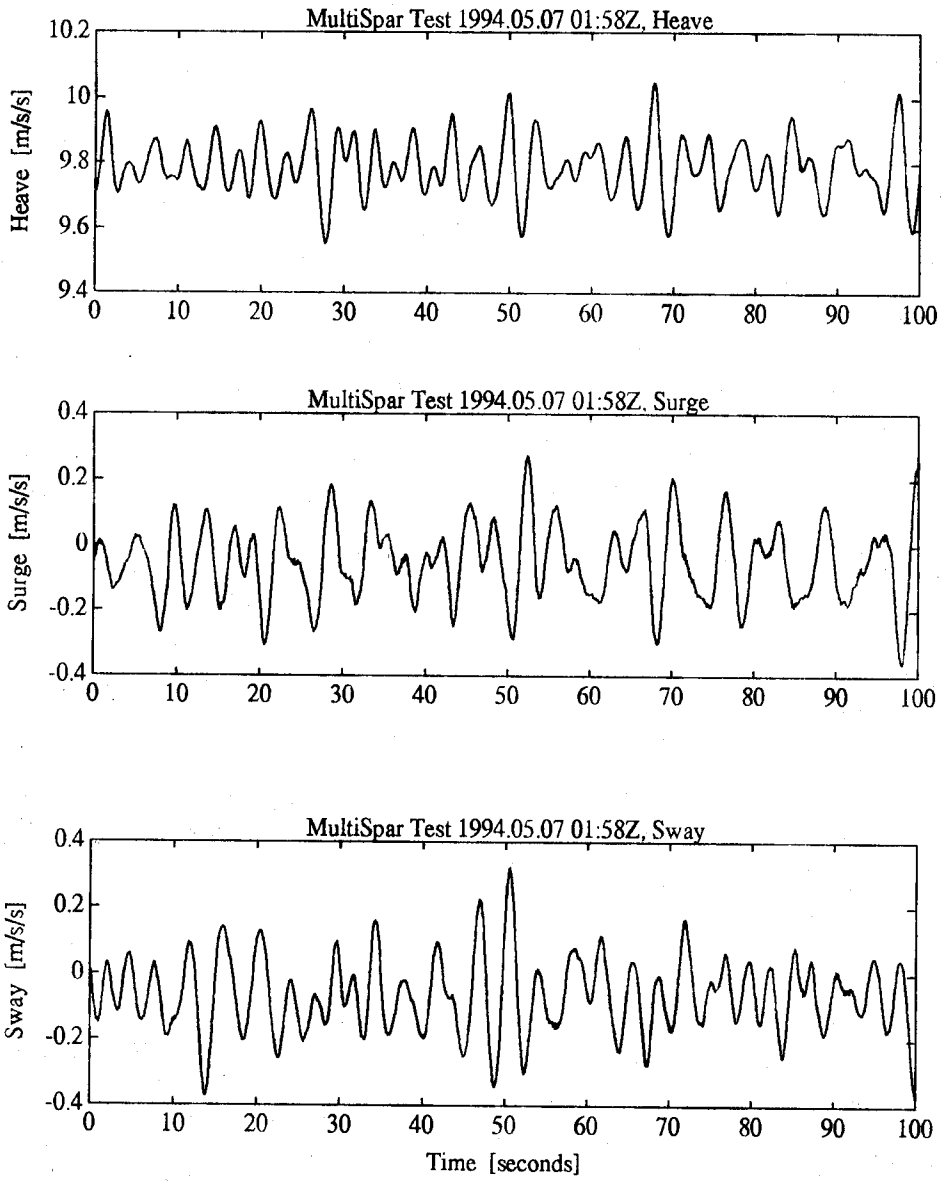

Figure 11: Concurrent measurements of time series for heave, surge and sway over a typical 100 second record.

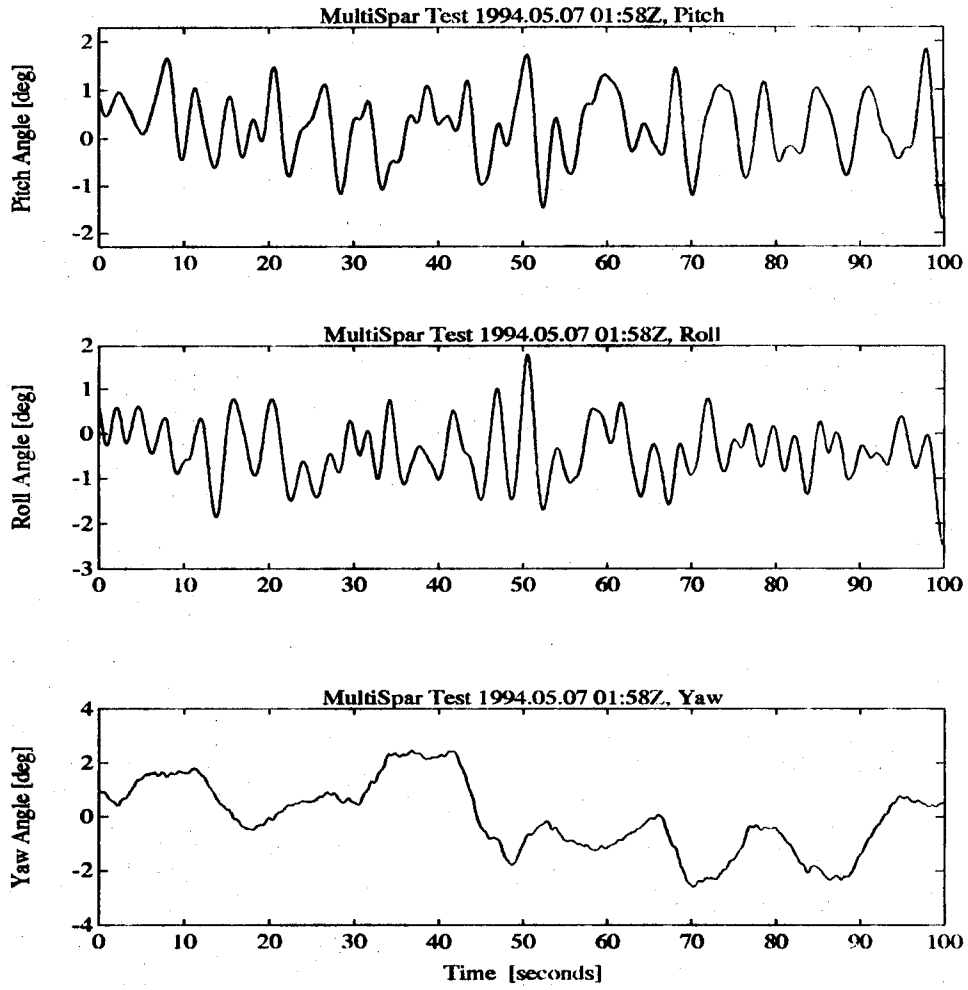

Figure 12: Concurrent measurements of time series for pitch, roll and yaw over a typical 100 second record.

phases and amplitude transfer functions are in Figures 14, 15, 16, and 17. In general, the response band-pass in pitching and rolling is much like the heave response except there is no overshooting and the response is at worst only 20% of the forcing. Once again, the transfer function is valid only where the coherence is high, so that the large values in the transfer function below 0.1 Hz are not significant.

The yaw response is very weak and is principally at lower frequencies than the waves. The buoy is symmetrical about its tether point so that the yawing is probably due to shifting currents.

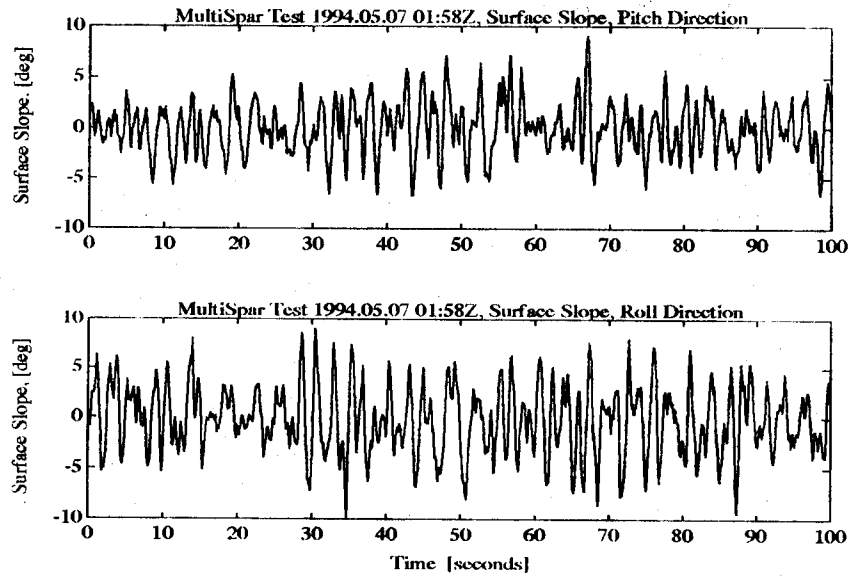

Figure 13: Concurrent measurements of time series for surface slope in pitch and roll directions over a typical 100 second record.

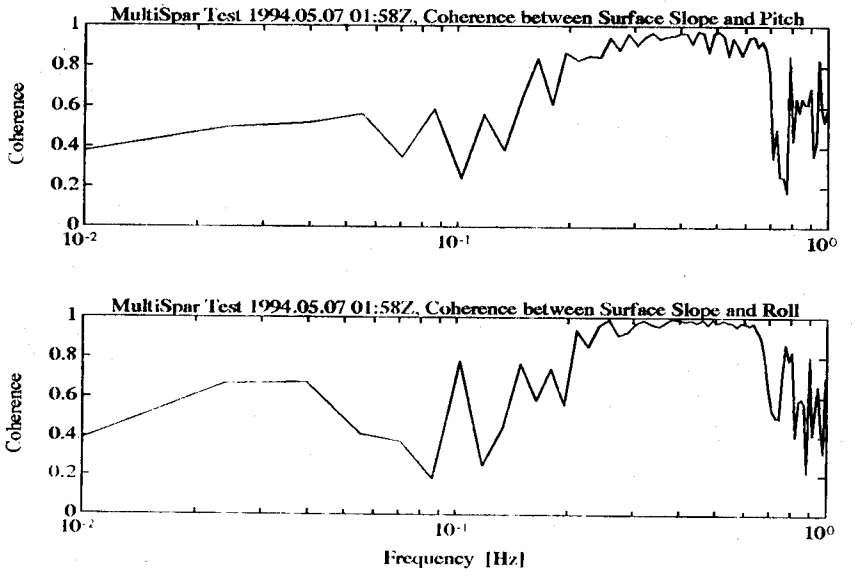

Figure 14: Coherence between surface slope and pitch (top panel) and surface slope and roll (bottom panel).

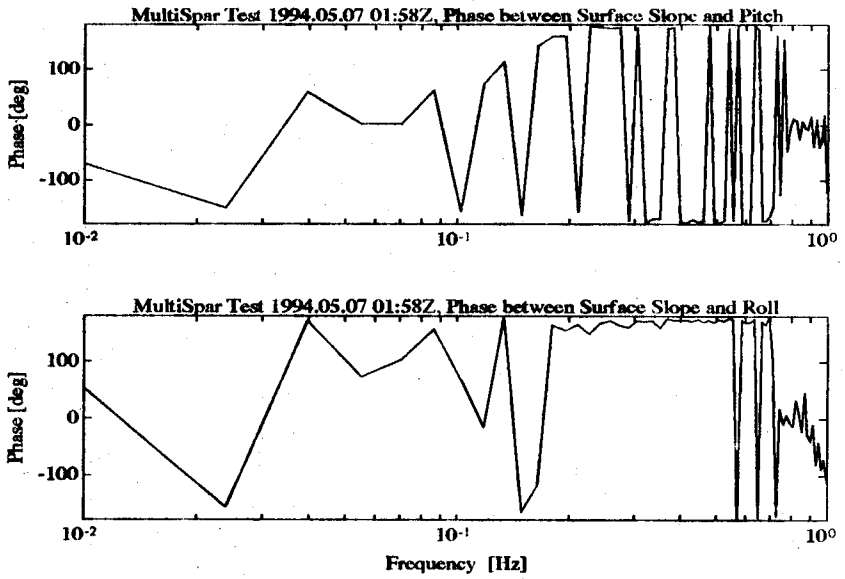

Figure 15: Phase between surface slope and pitch (top panel) and surface slope and roll (bottom panel).

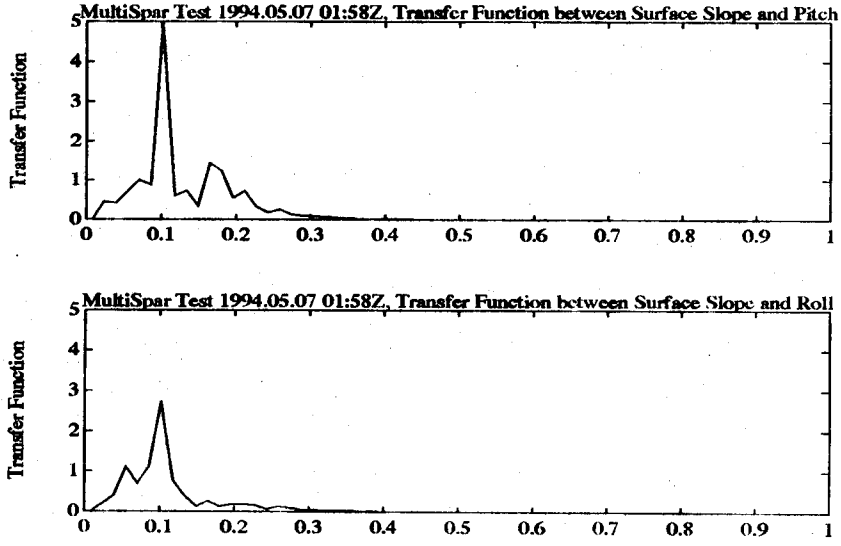

Figure 16: Transfer function between surface slope and pitch (top panel) and surface slope and roll (bottom panel) on linear scale.

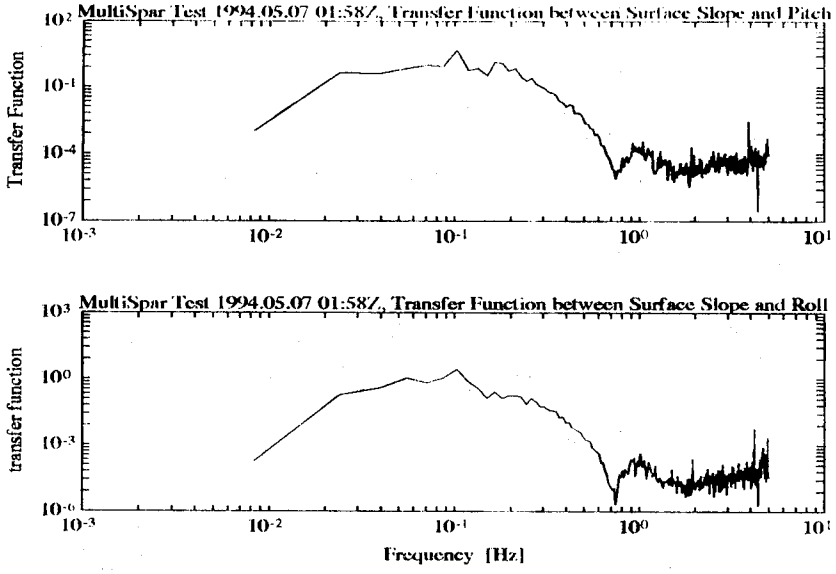

Figure 17: Transfer function between surface slope and pitch (top panel) and surface slope and roll (bottom panel) on log scale.

5.2 Wave and wind measurements

The time series from all eight wave staffs are shown in Figure 18 in two groups. The top panel in Figure 18 shows the six wave staffs that make up the centered pentagon of radius 92.7 cm and the bottom panel displays the three staffs near the centre at the apices of a right isosceles triangle of side 2.86 cm. In all cases the wave staff signals have been corrected for the motion of the buoy (Drennan *et al.* 1994).

A wave directional spectrum for a typical half-hour period is shown in Figure 19. It shows the windsea propagating to the west with remnants of an older windsea traveling the the southwest. The measured significant waveheight was 57 cm. The directional spectra have been computed with the maximum likelihood method using the six wave staffs that form the centered pentagon. The method followed is outlined in Drennan *et al.* (1994).

The wind components, as measured by the acoustic anemometer and corrected for the buoy's motion (Anctil *et al.* 1994), are displayed in the upper panel of Figure 20 and their spectra (25 minute average) in the lower panel. Note that the horizontal wind components have been rotated into the mean wind direction. All three components have -5/3 slopes at high frequencies as expected in the inertial sub-range.

The cospectrum of the downwind component of the stress is illustrated in Figure 21 (top panel) and the cumulative cospectra of u'w' (downwind) and v'w' (crosswind) are graphed in the bottom panel. In this case, the crosswind stress is near zero, so that the stress lies in the wind direction.

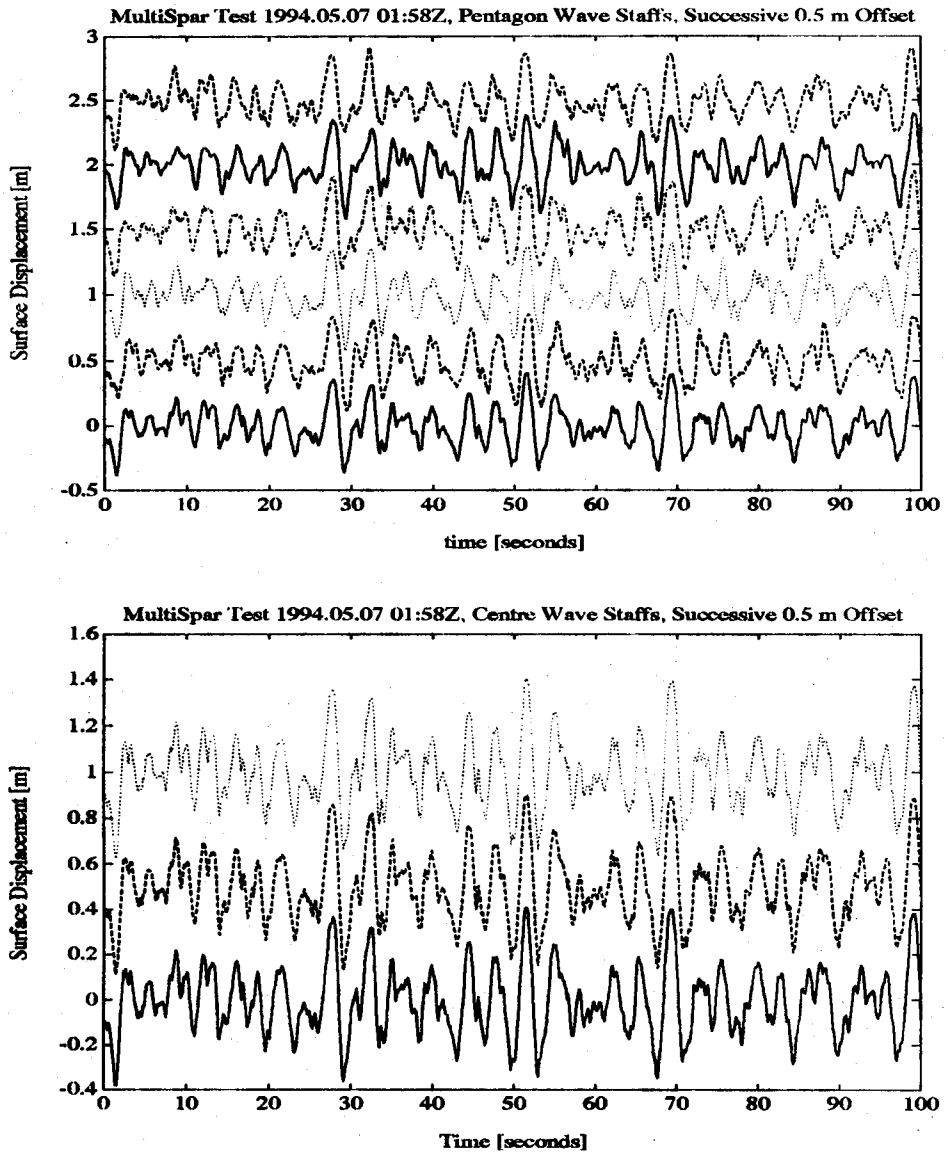

Figure 18: Concurrent time series of surface elevation for pentagon wave staffs (top panel) and center wave staffs (bottom panel).

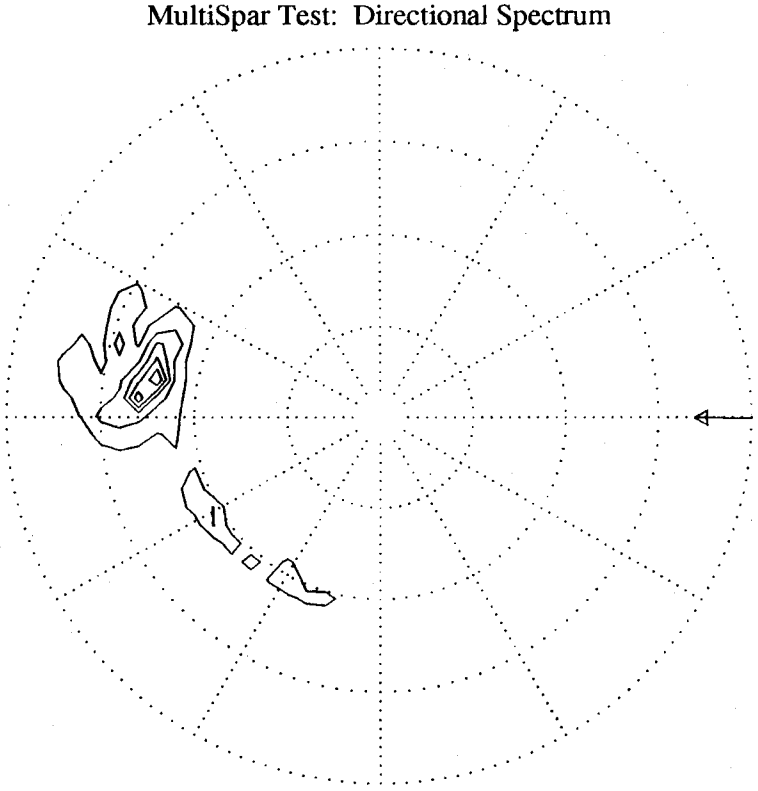

Figure 19: A typical directional wave spectrum computed from the six centered wave staffs using the MLM method. Data are presented in geophysical coordinates with grid lines 30° apart. Frequency spacing is 0.1 Hz to a maximum of 0.4 Hz. The wave energy is shown in the direction of propagation, with equally spaced contours normalized to the maximum energy. The arrow shows the wind direction.

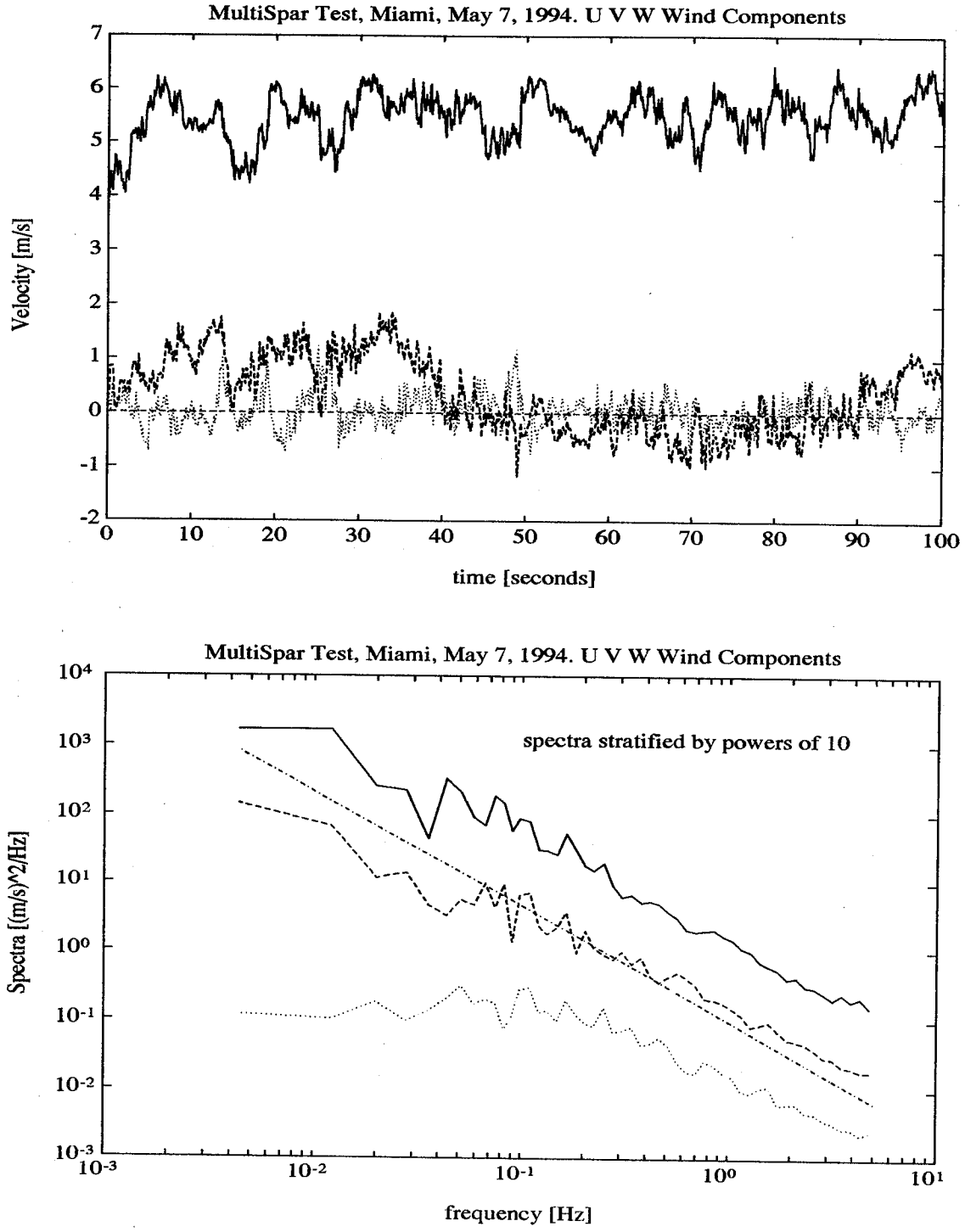

Figure 20: Time series of wind components from sonic anemometer over a 100 second record (top panel) and the corresponding spectra averaged over a 25 minute record (bottom panel).

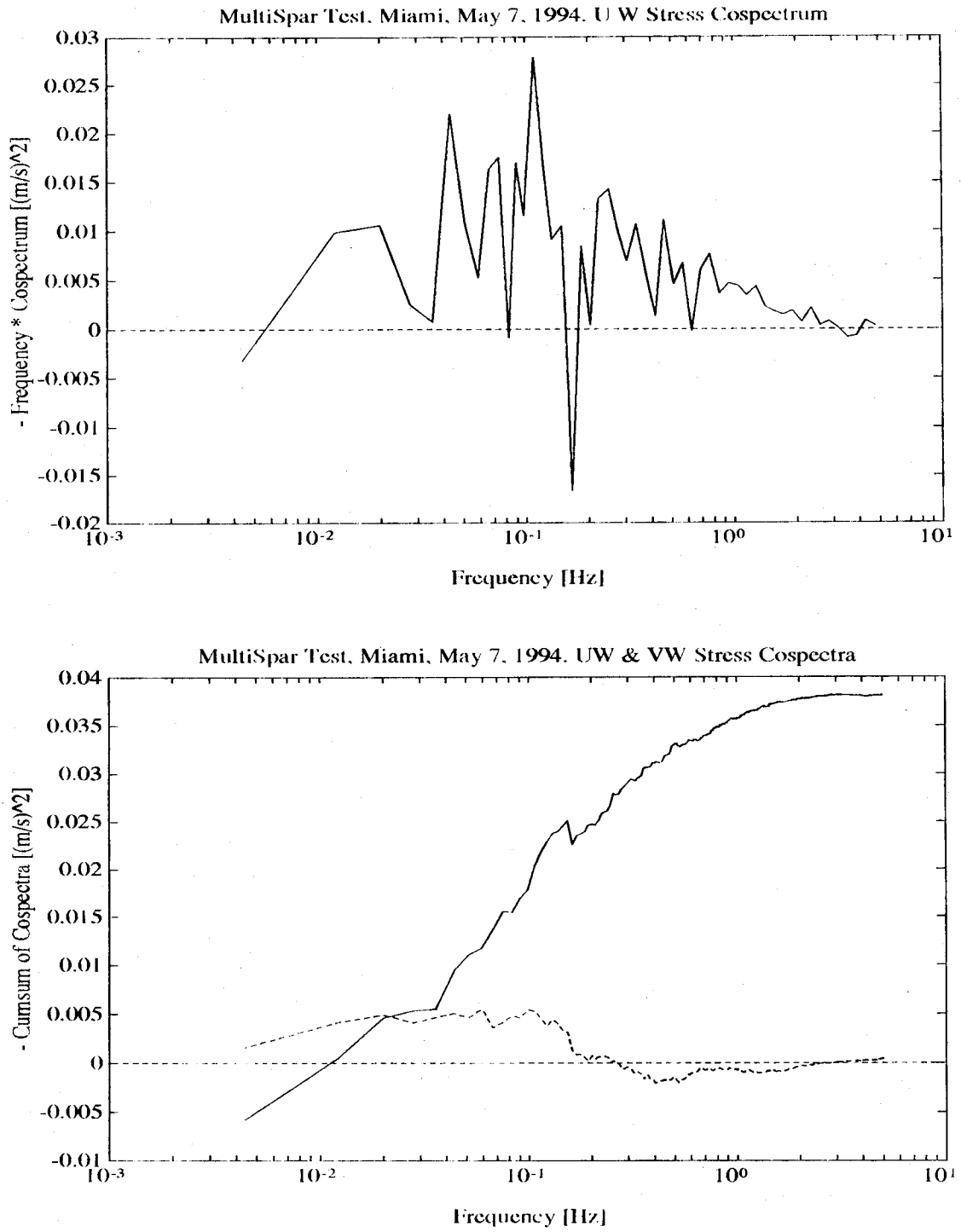

Figure 21: Cospectrum of downwind component of the stress (top panel) and the cumulative cospectra of the downwind and crosswind components (bottom panel).

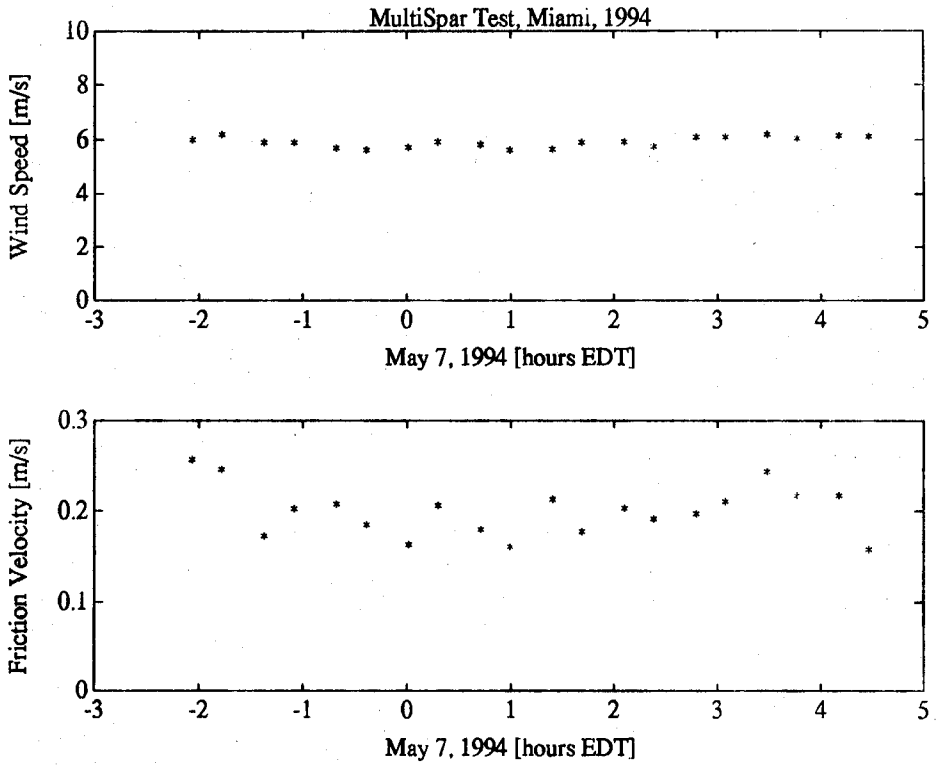

Figure 22: Discrete time series of wind speed (top panel) and friction velocity (bottom panel) from sonic anemometer at 25 minute intervals.

Finally we examine the history of wind speed and stress throughout the test in Figure 22. The wind was remarkably steady and the stress (here indicated by the friction velocity) shows the usual variability of second order turbulence products.

6 SUMMARY

A new general purpose, modular, lightweight buoy platform was designed for air-sea interaction studies. The design concept was driven by the need for high-resolution directional wave measurements over a wide range of wavelengths and for accurate measurements of air-sea fluxes coincident with wave observations and other relevant parameters in the upper ocean layer. These considerations required a stable platform and led to a choice of a spar-like buoy. Furthermore, the constraints that the buoy behave like a stable platform for short gravity waves and exhibit surface-following characteristics for longer wave motion led to an innovative design consisting of several spar members along the perimeter of an open cage. This MultiSpar arrangement provides not only the desired stability characteristics, but also a structure open and unobtrusive to measurements of atmospheric and oceanic variables. The buoy can accept flexible sensor systems to address diverse fields of research in oceanography and air-sea interaction.

The buoy can be deployed in a drifting mode to acquire observations along Lagrangian trajectories or in a tethered mode to acquire long time series observations. In the tethered mode, additional or complementary sensors could be assembled on the Tether buoy.

The complete buoy system was field tested in the Atlantic coastal waters off Miami, Florida. The sea trials have demonstrated the sea worthiness of the buoy system in low to moderate wind and sea conditions. Measured response functions coupled with design calculations indicate that the buoy will function well in long waves as well. Although the flux and wave observations were limited, they nevertheless show the quality and capability of the MultiSpar buoy to provide high-resolution and accurate directional wave and surface flux measurements in open ocean conditions.

7 REFERENCES

Anctil, F., M.A. Donelan, W.M. Drennan and H.C. Graber, 1994: Eddy correlation measurements of air-sea fluxes from a discus buoy. *J. Atmos. Ocean. Technol.*, **11**(4), 1144-1150.

Berteaux, H.O. and R.G. Walden, 1978: Design of a Stable Floating Platform for Air-Sea Interaction Measurements. *Woods Hole Oceanographic Institution Technical Report*, **WHOI-78-88**, 73pp.

Cardone, V.J., H.C. Graber, R.E. Jensen, S. Hasselmann, and M. Caruso, 1995: In Search of the true surface wind field in SWADE IOP-1: Ocean Wave modelling perspective. *Global Atmos. Ocean Sys.*, (In press).

Crowther, P.A. and I.R. Perry, 1970: Measurements of Sea Surface Roughness Statistics for Various Windspeeds. *British Admiralty Report*, **ND(F) 194**, 23pp.

Donelan, M.A., J. Hamilton and W.H. Hui, 1985: Directional spectra of wind-generated waves. *Phil. Trans. R. Soc. Lond.*, **A 315**, 509-562.

Drennan, W.M., M.A. Donelan, N. Madsen, K.B. Katsaros, E.A. Terray and C.N. Flagg, 1994: Directional wave spectra from a Swath ship at sea. *J. Atmos. Ocean. Technol.*, **11**(4), 1109-1116.

Graber, H.C., M.W. Byman and W. Rosenthal, 1990: Numerical Simulation of Surface Wave Refraction in the North Sea. Part 1: Kinematics. *Dt. Hydrogr. Z.*, **43**, 1-18.

Graber, H.C., M.W. Byman and H. Gunther, 1992: Numerical Simulations of Surface Wave Refraction in the North Sea. Part 2: Dynamics. *Dt. Hydrogr. Z.*, **44**, 1-15.

Herr, F., C. Luther, G. Marmorino, R. Mied and D.R. Thompson, 1991: Science Plan for the High Resolution Remote Sensing Program, *Office of Naval Research*, Arlington, VA 17 pp.

Katsaros, K.B., M.A. Donelan and W.M. Drennan, 1993: Flux measurements from a Swath ship in SWADE. *J. Mar. Sys.* **4**, 117-132.

Shay, L.K., P.C. Zhang, E.J. Walsh, and H.C. Graber, 1995: Simulated surface wave-current interactions during SWADE. Revision submitted to *Global Atmos. Ocean Sys.*

Steele, K.E., C.-C. Teng and D.W.C. Wang, 1992: Wave direction measurements using pitch-roll buoys. *Ocean Engng.*, **19** (4), 349-375.

Walsh, E.J., L.K. Shay, H.C. Graber, A. Guillaume, D. Vandemark, D.E. Hines, R.N. Swift, and J.F. Scott, 1995: Observed surface wave-current interactions during SWADE. Revision submitted to *Global Atmos. Ocean Sys.*

Weller, R.A., M.A. Donelan, M.G. Briscoe and N.E. Huang, 1991: Riding the crest: A tale of two wave experiments. *Bull. Amer. Met. Soc.*, **72**, No. 2, 163-183.

Zdravkovich, M.M., 1981: Review and classification of various aerodynamic and hydrodynamic means for suppressing vortex shedding. *J. Wind Eng. Industr. Areodyn.*, **7**, 145-189.

REPORT DOCUMENTATION PAGE

Form Approved
OMB No. 0704-0188

1. Agency Use Only *(Leave blank).*	2. Report Date. October 1995	3. Report Type and Dates Covered.

4. Title and Subtitle.

A LIGHTWEIGHT MULTI-SPAR BUOY
-- DESIGN AND SEA TRIALS --

5. Funding Numbers.

Program Element No.

N00014-91-J-4142

Project No.

Task No.

Accession No.

6. Author(s).

Hans C. Graber, Eugene A. Terray, Mark A. Donelan,
John VanLeer, and William M. Drennan

7. Performing Organization Name(s) and Address(es).

See reverse.

8. Performing Organization Report Number.

RSMAS Tech. Rept. 95-009

9. Sponsoring/Monitoring Agency Name(s) and Address(es).

Office of Naval Research
Remote Sensing Program (Code 321 RS)
800 North Qunicy Street
Arlington, VA 22217-5000

10. Sponsoring/Monitoring Agency Report Number.

11. Supplementary Notes.

12a. Distribution/Availability Statement.

Approved for public release;
distribution unlimited

12b. Distribution Code.

13. Abstract *(Maximum 200 words).*

There is a growing need for high resolution wave directional measurements at sea, arising in diverse fields such as wave dynamics, microwave and acoustic remote sensing, air-sea coupling and gas transfer. This report describes the design and sea trials of a *general purpose lightweight spar* with wave and surface flux measurement capabilities. The chosen design led to a short spar. Instead of intersecting the surface as a single column, a pentagonal cage of slender cylinders separated by several meters is used. The MultiSpar is laterally tethered to a surface mooring which itself can carry both air- and water-side sensors and telemetry. The flexible design concept of this MultiSpar buoy is amenable to measurements in the open ocean, in boundary currents, on the continental shelf and in coastal waters. The first results of a prototype MultiSpar buoy are presented from sea trials conducted off Miami, Florida in May 1994. Measurements include wind stress and directional wave spectra from a nested wave gauge array.

14. Subject Terms.

Spar buoy
Air-sea interaction
Wind stress
Wave dynamics
Wave spectrum
Remote sensing

15. Number of Pages. 38

16. Price Code.

17. Security Classification of Report.	18. Security Classification of This Page.	19. Security Classification of Abstract.	20. Limitation of Abstract.
UNCLASSIFIED	UNCLASSIFIED	UNCLASSIFIED	

7. (concluded)

Division of Applied Marine Physics
Division of Meteorology and Physical Oceanography
Rosenstiel School of Marine and Atmospheric Science
University of Miami, Miami, FL 33149-1098, USA
Department of Applied Ocean Physics and Engineering
Woods hole Oceanographic Institution, Woods Hole, MA 02543, USA
National Water Research Institute
Department of Environment
Canada Centre for Inland Waters, Burlington, Ontario, L7R 4A6, Canada